Particle Accelerators, 1987, Vol. 21, pp. 29–42
Photocopying permitted by license only

Printed in the United States of America

SKY- AND GROUNDSHINE PHENOMENA AND RELATED RADIOLOGICAL QUANTITIES EVALUATED FOR THE ENVIRONMENT OF A HIGH-CURRENT SPALLATION FACILITY

J. M. ZAZULA,† D. FILGES, and P. CLOTH

Institut für Reaktorentwicklung, Kernforschungsanlage Jülich GmbH, Postfach 1913, D-5170 Jülich, West Germany

(Received July 25, 1985; in final form May 9, 1986)

Secondary radiation propagation has been evaluated for the environment of a spallation facility, which was modelled in a two-dimensional cylindrical geometry. The high-energy particle transport Monte Carlo code HETC, based on the intranuclear cascade-evaporation model, was used to provide secondary-neutron energy spectra and angular distributions from a thick ^{238}U target bombarded by a 1.1-GeV, 5-mA proton beam. The two-dimensional DOT 4.2 discrete-ordinates S_N transport code was run to calculate the penetration of neutrons and secondary gammas through the bulk shielding, earth, and atmosphere. Results important for radiation protection at the facility, including secondary particle fluxes, dose equivalents, absorbed doses and induced radioactivity, were determined using previously released data for high-energy neutron, secondary-particle energy release, and residual nuclei production, together with the ENDF-B/IV data for low energies. The sky- and groundshine effects were found to be similar to the measurements around other high-energy accelerators, with the initial build-up factor of 2.5 at a distance of about 60 m from the bulk shielding of the facility, 1.5 m below ground level. An attenuation length of about 150 m in air was also estimated. The induced radioactivity by secondary radiation in air and water exceeds the maximum permissible concentrations only inside the station at positions close to the source.

1. INTRODUCTION

Increased neutron and gamma radiation fields have been observed[1,2] in the vicinity of accelerator facilities, which may pose a radiation hazard for laboratory staff and surrounding populations. The spatial distribution of the external dose levels are usually affected by the so-called sky- and groundshine effects,[1–5] due to backscattering of the secondary radiation from the ground, atmosphere, and neighboring buildings. Another problem is caused by possible contamination of the surrounding air and ground water by the induced radioactivity.

Numerous radiation protection problems were studied in the course of the Spallation Neutron Source Project (SNQ),[6] which was planned at Kernforschungsanlage Jülich (KFA). The neutron yields and neutron fluxes of a depleted uranium (0.2 wt% ^{235}U) target bombarded by a 1100-MeV, 5-mA proton beam were considered. Neutron and secondary-gamma transport through the shielding

† On leave from the Institute of Nuclear Physics, Krakow, Poland

and in the vicininty of the target up to 1.5 km from the target station was calculated.

To estimate exposures to high-energy radiation, Monte Carlo simulation[6–8] of the hadronic cascade process is usually performed. Unfortunately, this method is restricted to regions close to the target assembly. Also, methods based on a semiempirical attenuation formula—e.g., the ray-through-layout algorithm[9]—developed for the SNQ shielding design could not account for albedo effects and the neutron spectra transition between different media. Therefore, for problems with large spatial range, such as the one posed here, Monte Carlo–type high-energy neutron source calculations, coupled with a two-dimensional discrete-ordinates solution (e.g., the DOT 4.2 code[10]) of the neutron transport equation (see Section 2) remain the only possible calculation approach.

This approach neglects the transport and dose contributions of charged particles such as protons, pions, and heavy ions produced by the primary protons and secondary neutrons in the target and shielding. These particles are slowed down and absorbed within spatial distances small compared with the thickness of shielding against neutrons. The benchmark calculations of Alsmiller *et al.*[11] and the previous work of Zazula *et al.*[12] have shown that for bulk shielding the influence of particles other than the neutrons in the hadronic cascade becomes neglibigle, particularly when compared with the statistical accuracy of the Monte Carlo method applied to deep-penetration problems. Also, the development of intense electromagnetic cascades from pion and muon decay is negligible at a 1100-MeV beam energy, the energy of the SNQ accelerator system.

The limiting requirement of the method applied here is given by the relevant transport cross section and response function data for high-energy neutrons. The system of computer codes and data files that we used is described in the next section. The estimated results for radiation flux, dose equivalent, absorbed dose, and induced radioactivity are discussed in Sections 3 and 4.

2. DETAILS OF THE CALCULATION

The analysis involved the following:

(i) Space, energy, and angular distributions of the secondary-radiation source produced by irradiation of the target and other materials by the proton beam.
(ii) Description of the transport process of the secondary radiation through the shield, ground, and atmosphere.
(iii) Application of the response functions relevant to the radiation interaction with elements of the environment, human tissue, radiometric counters, etc.

The INCE-model (intranuclear cascade-evaporation)[6–8] was the basis for evaluating the source term. Then, the discrete-ordinates multigroup S_N method[10] was used to solve the transport problem. The high-energy part of the response functions was previously obtained[12] using a single-collision option of the INCE model. The implemented code system is shown in Fig. 1.

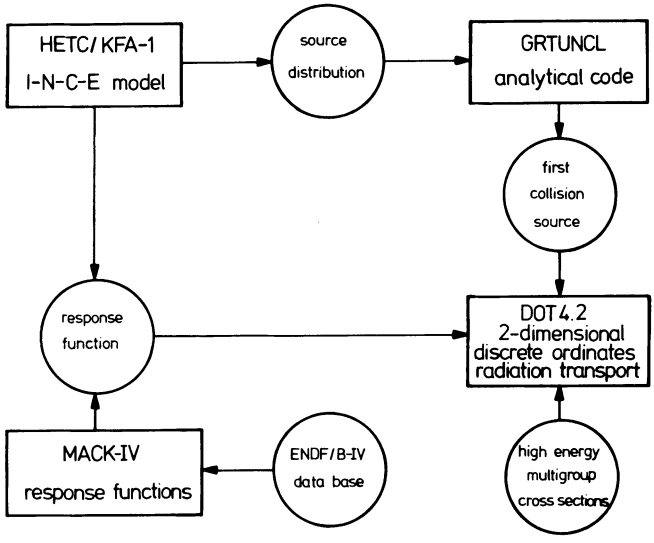

FIGURE 1 Schematic of the computer code system.

To provide secondary-neutron yields and the source term, the KFA version of the Monte Carlo code HETC[8] was run for a three-dimensional model[6] of a ^{238}U target with water cooling and aluminium cladding. The target consists of a material mixture of depleted uranium, aluminium, and water, designed as a spinning wheel 2.5 m in diameter and 10 cm thick. The proton beam hits the 10-cm-high circumference of the spinning wheel. The energy spectrum of the neutrons produced in the forward direction (the beam direction) is shown in Fig. 2. For the deep-penetration transport calculation, the beam channel and complex target structures were neglected. The source term, which was calculated with HETC and derived from the history tapes with an analysis code called SIMPEL,[8] was provided to the 2-D transport S_N code as an equivalent volume-integrated neutron point source with a multigroup energy structure and an S_N angular distribution. This point source was then input to the GRTUNCL code,[10] yielding a first-collision neutron source, distributed over the whole mesh grid of finite space cells used in the discrete-ordinates transport calculation. Azimuthal symmetry of the source was assumed, with the beam direction representing all azimuthal angles. The angular anisotropy was taken into account only for different vertical angles relative to the primary protons. To perform the deep-penetration transport calculation, the 2-D DOT 4.2 discrete-ordinates code[10] was run.

The SNQ facility was modeled in cylindrical "r–z" geometry, as shown in Fig. 3, taking the beam direction as the axis and the vertical direction above the source as the z axis. The target station consisted of the 5.5-m-thick iron shielding, surrounding by a 1-m-thick concrete layer. A graphite moderator 2 m high and 3 m in diameter was placed above the target. The total height of the building was 6.5 m above ground level, and we assumed a depth of 3.5 m below ground. The atmosphere and the ground surface up to 1.5 km from the facility, both radially

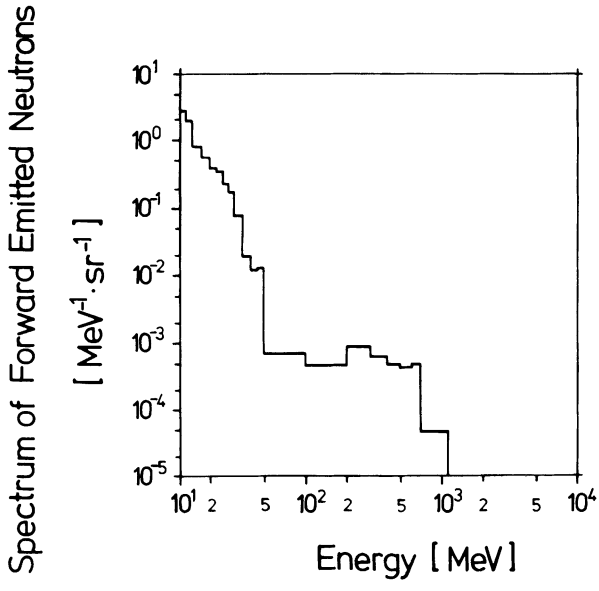

FIGURE 2 Energy spectrum of secondary neutrons produced in the forward direction from the spallation target.

and vertically, were included in the calculation. A spatially varying mesh grid was used, with the size of a single cell 0.5 m inside the shield and 200 m in the air. Therefore, a total of 32×25 meshes was used.

The materials used in the calculations are listed in Table I. The so-called LAHI multigroup neutron cross section library,[9] a KFA combination of the ORNL[13] and LANL[14] libraries, was used for the calculations. The library contains 53

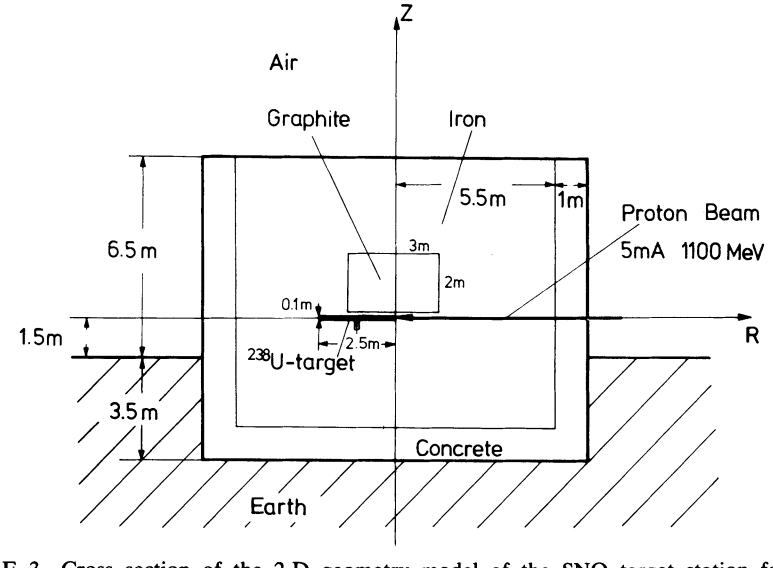

FIGURE 3 Cross section of the 2-D geometry model of the SNQ target station for DOT 4.2 calculations.

TABLE I

Material Composition Used in the Calculations

Material	Nuclide density (atom/barn-cm)						
	H	C	N	O	Al	Si	Fe
Iron	—	—	—	—	—	—	8.60×10^{-2}
Concrete	3.86×10^{-3}	—	—	4.54×10^{-2}	4.82×10^{-4}	2.08×10^{-2}	1.07×10^{-3}
Earth	6.02×10^{-3}	—	—	3.73×10^{-2}	—	1.72×10^{-2}	—
Air	—	—	4.33×10^{-5}	1.07×10^{-5}	—	—	—
Graphite	—	9.03×10^{-2}	—	—	—	—	—

neutron groups in the energy range from 1×10^{-4} eV to 800 MeV and 21 gamma groups between 0.01 and 14 MeV. To cover the whole energy range up to 1100 MeV, the highest energy group in LAHI (700–800 MeV) was uniformly extended to 1100 MeV. This is a fairly good extrapolation, because in the whole energy range from 700 to 1100 MeV, the values of total cross section, within-group scattering cross section, and downscattering cross section can be assumed constant and corresponding to the mean value between 700 and 800 MeV. The approximately constant character of high-energy neutron cross sections has previously been confirmed[12] by INCE model calculations.

The neutron source spectrum from the target was integrated over the groups, taking the first interval between 700 and 1100 MeV. It should also be noted that the ^{14}N data were separately retrieved from the ORNL–HILO library,[13] collapsed to the LAHI multigroup structure, extended in energy, and revised for the elastic scattering cross section. A P_3-order Legendre expansion of the cross section data was available. A S_8 angular quadrature set was used in the DOT 4.2 calculations, with 48 directions representing the higher angular anistropy above 1 MeV, and S_4 with 16 discrete directions was assumed to be a fairly accurate representation below 1 MeV, down to thermal energy. Options for coarse mesh rebalances and zone-dependent error importances were applied using the acceleration techniques of the DOT 4.2 code. In the production runs, an iteration convergence of about 3%—much better in the keV energy range—could be reached within the limit of 100 inner iterations per group. The run time on an IBM 3033 was typically about 23 minutes.

The space- and energy-dependent neutron and gamma fluxes obtained by DOT were folded with the group-averaged response functions, representing

(i) Reaction rates, expressed as the product of flux and reaction cross sections
(ii) Secondary particle yields, expressed as the product of neutron flux and production cross sections
(iii) Induced radioactivity, expressed as the product of flux and cross sections for production of radioactive residual nuclei
(iv) Absorbed dose, expressed as the product of flux and kerma factors (see Section 4)
(v) Dose equivalent, expressed as the product of flux and the conversion factors, taken from the literature.[15]

Response functions below 20.0 MeV were taken from the MACKLIB–IV library,[16] based on the ENDF/B-IV neutron data files. Above 20 MeV, the reaction cross sections were obtained[12] using the HETC code and analysis of the single-neutron collisions with nuclei of isotopes which are of shielding or biological importance. An analysis code for HETC history tapes was written to process these data into multigroup activity tables. The basic procedure and the results were published in Ref. 12.

3. RADIATION LEVELS OUTSIDE THE SHIELD AND ITS PROPAGATION

From a radiation hazard point of view, the total neutron dose plus the gamma dose outside the shielding are of interest. The estimates outside the SNQ target station, at beam level (1.5 m above ground) and 6.75 m away from the external concrete wall, in the earth (0.25 m below the ground), and above the building (7.5 m below the roof) are shown in Table II. The height dependence of the total dose equivalent in the first radial interval outside the shielding is shown in Fig. 4, and the radial dependence in the first vertical interval above the roof is shown in Fig. 5. In Fig. 4, one can observe the horizontal maximum due to the forward (with respect to the beam) anisotropy of the neutrons emitted from the target. The increasing trend of the dose near the roof level is caused by streaming of radiation from the highly exposed region above, due to replacement of a part of the iron bulk shielding by the graphite moderator, which does not protect as efficiently against high-energy neutrons as does iron. Therefore, one may conclude from the calculations that for the 90° direction with respect to the beam the residual 3 m of iron above the moderator do not ensure a sufficient roof shielding and might cause the radiation protection limits (0.5 mrem per hour) to be exceeded by three orders of magnitude.

The next problem is the propagation of the radiation from the source at the external shielding limits through the air-over-ground environment of the SNQ

TABLE II

Total Dose Equivalent Estimates in mrem/hr on the Surface Outside the SNQ Target Station for a Depleted Uranium Target Bombarded with 1100-MeV, 5-mA Protons

	Total dose equivalent estimate (mrem/hr)		
Contribution	At beam level	Below ground level	At the roof
Neutrons <20 MeV	5.86	3.05	406
Neutrons >20 MeV	6.51×10^{-4}	1.10×10^{-3}	7.62×10^{-2}
Total gammas	1.43	0.62	15.6
Total	7.28	3.67	422

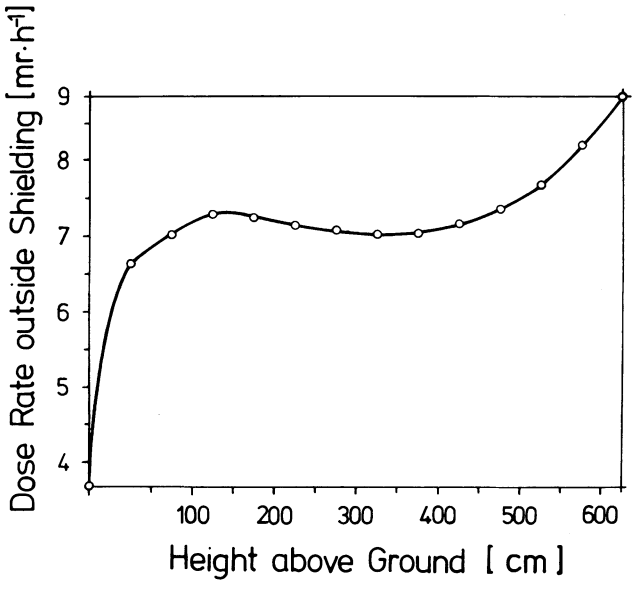

FIGURE 4 The dose rate at the side of the shielding (first radial mesh interval) versus height above ground.

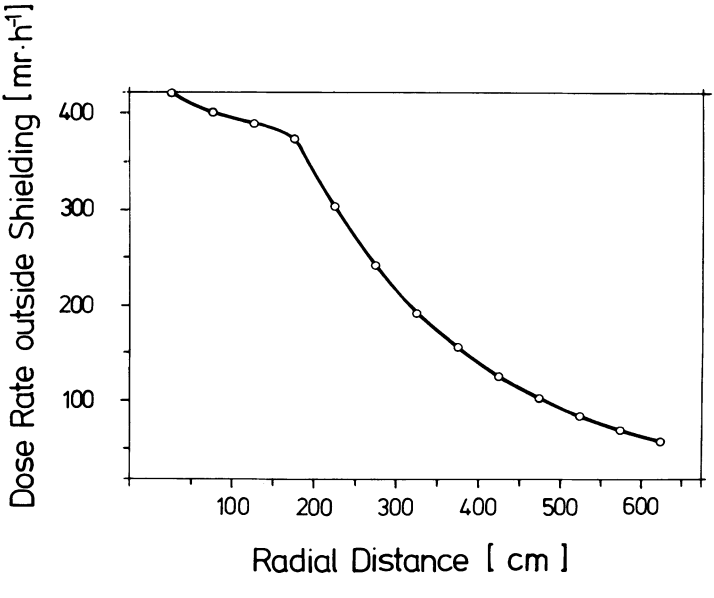

FIGURE 5 The dose rate above the roof (first vertical mesh interval) versus radial distance.

spallation facility. Up to a distance of 100 m from the station, it is not possible to describe the decrease of the radiation levels proportional to $1/4\,\pi r^2$ or by an attenuation proportional to $\exp(-x/\lambda)$. The secondary particle radiation exhibits the initial build-up of a factor of about 2.5 at a distance of about 60 m followed by an exponential decrease with an attenuation length of about 250 m. Similar behavior of the fast neutron flux and of the dose equivalent was previously reported[2] from measurements around the high-energy accelerators at the CERN, BNL, DESY, and Rutherford laboratories. A build-up factor between 2.5 and 7.0 was found, together with build-up distances between 100 and 150 m, and attenuation lengths between 200 and 1000 m. The build-up phenomenon is the result of the well-known sky- and groundshine effects.

By contrast, the initial increase does not occur for the calculated vertical dependence curve of the dose equivalent, as compared with to the horizontal dependence curve (see Fig. 6). Therefore, the build-up effect seems to be strongly connected to the ground albedo, which affects the horizontal values more than the vertical ones. Numerical fits of the results with semiempirical formulas[2] developed for the description of the skyshine effect were not performed here, since in our opinion such expressions do not have a universal character and are strongly dependent on the source energy and the geometry detals of the facilities considered.

Some significant differences are observed between the asymptotic long-distance behavior of the flux, dose equivalent dose absorbed in air, and induced radioactivity in air. These results are compared in Fig. 7 for the horizontal direction and in Fig. 8 for the vertical direction. The differences of the

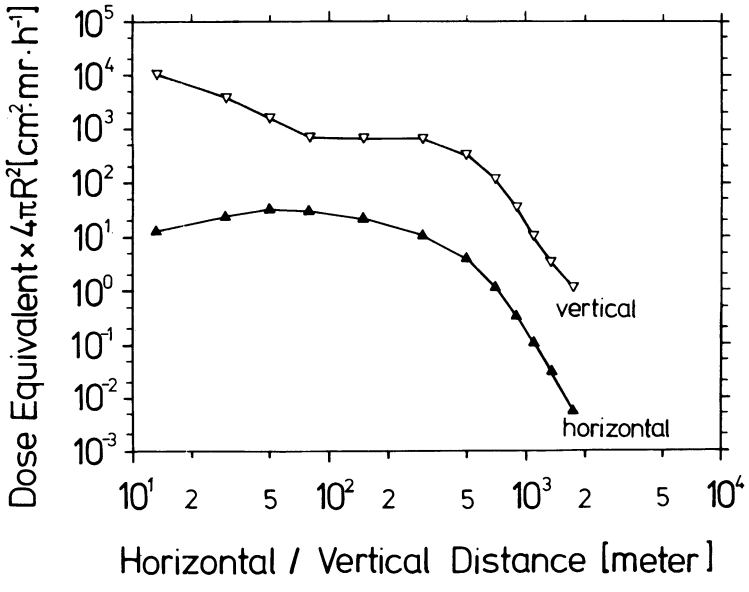

FIGURE 6 Comparison of the horizontal and vertical dependence of the dose equivalent around the SNQ shielding.

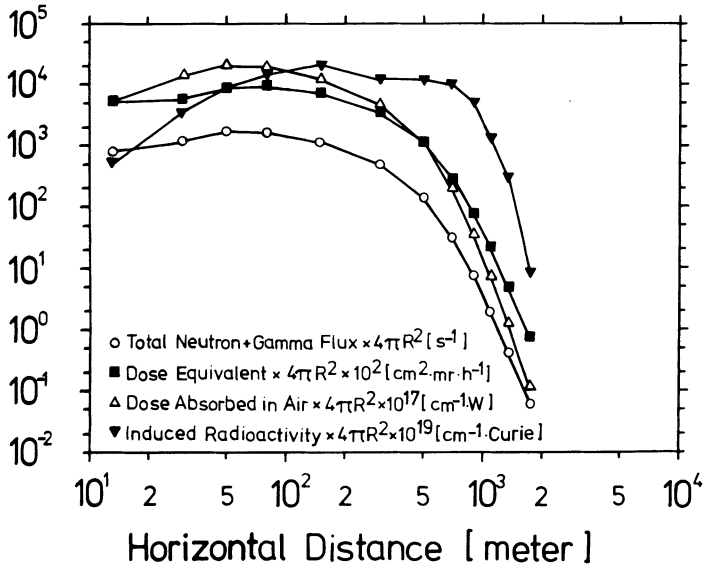

FIGURE 7 The flux, dose equivalent, absorbed dose, and induced radioactivity in air at beam level versus horizontal distance from the SNQ station.

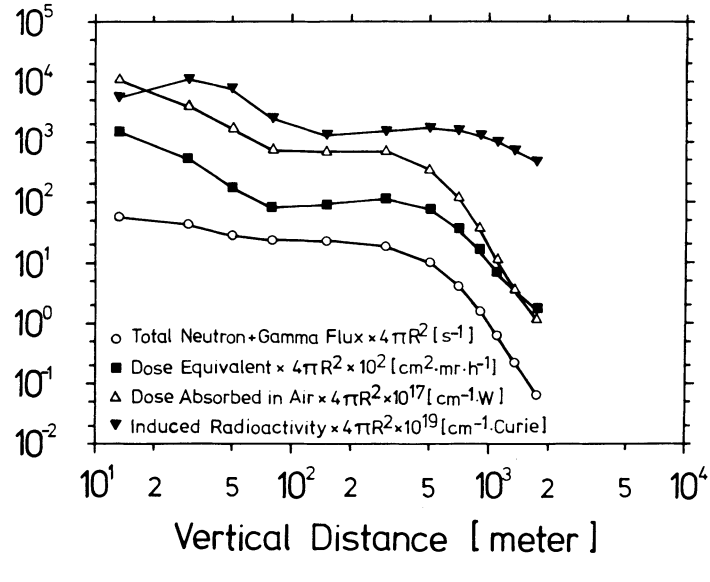

FIGURE 8 The flux, dose equivalent, absorbed dose, and induced radioactivity in air versus height above the SNQ station.

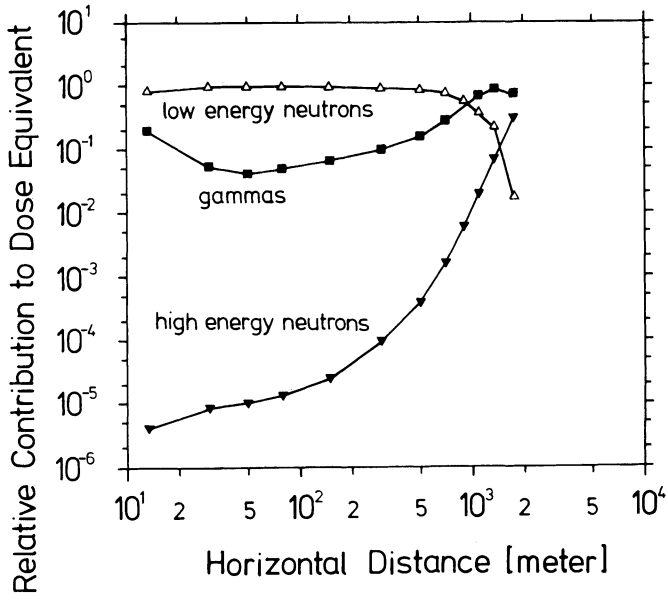

FIGURE 9 Relative contributions to the dose equivalent of high-energy neutrons (>20 MeV), low-energy neutrons (<20 MeV), and gamma particles versus horizontal distance from the SNQ station.

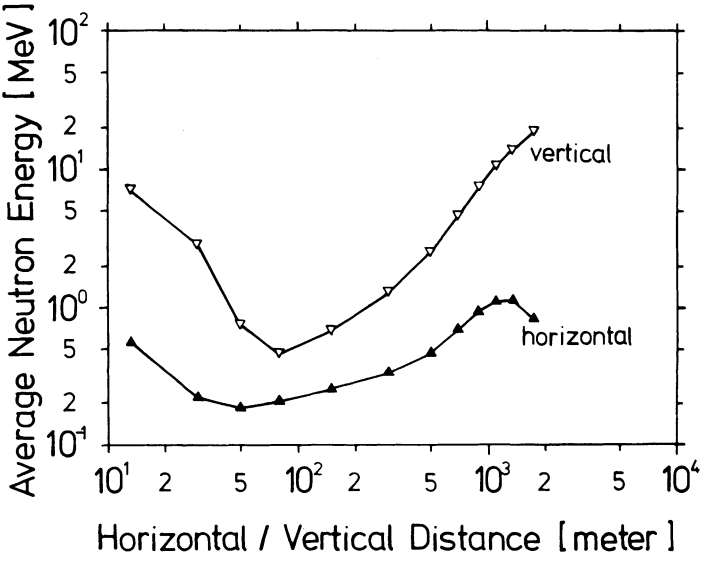

FIGURE 10 Average energy of skyshine neutrons versus distance from the SNQ station.

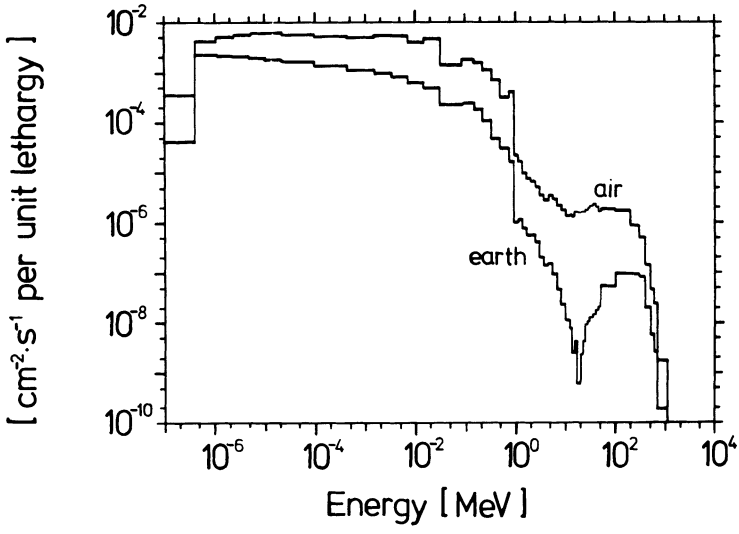

FIGURE 11 Average neutron energy spectra in the air and earth.

attenuation lengths are caused by the different energy ranges of the secondary particles at different distances. To explain this behavior, the contributions to the dose equivalent from the different kinds of secondary radiation is compared in Fig. 9. The neutron spectrum distribution in air is equal to the distribution of neutrons at the surface of the shielding, and thus, the low-energy neutrons dominate. Farther away these slow neutrons are absorbed, and the fast neutrons, penetrating large distances (hundreds of meters) in air, are not slowed down

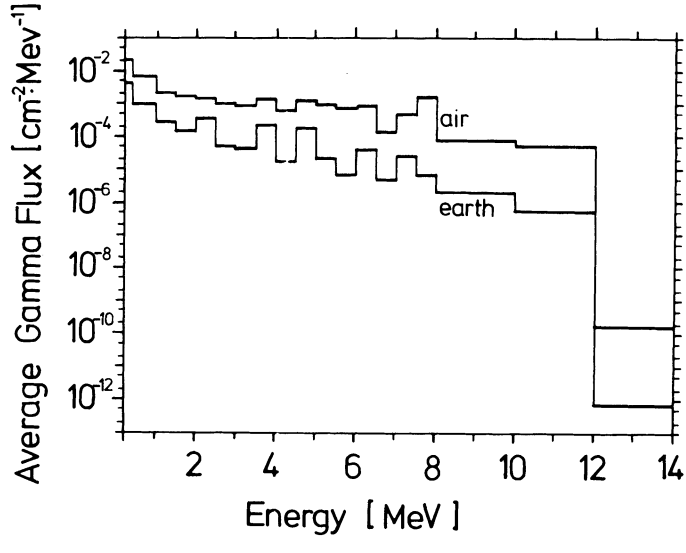

FIGURE 12 Average gamma particle energy spectra in the air and earth.

much. Thus, at a distance of about 1000 m and more, the high-energy neutron and gamma components contribute more to the dose. This hardening of the skyshine radiation spectrum was also described by Rindi and Thomas.[2] This effect is shown in Fig. 10. The gamma component decreases somewhat more slowly than the neutron component, because secondary photons are produced by thermal neutron capture of the light nuclei of air and earth. The energy spectra, averaged over the volumes of air and ground, are shown for neutrons in Fig. 11 and for gammas in Fig. 12.

4. ABSORBED DOSE AND INDUCED RADIOACTIVITY

With the previously evaluated charged-particle energy release and residual nuclei production data[12] for high-energy neutrons, it is possible to estimate the energy deposition and the induced radioactivity in shielding and moderating materials, assuming that the neutrons and photons, as the most penetrating components, dominate the secondary radiation spectrum around the spallation source. In areas very close to the high-power target, these estimates were separately determined.[6] The kerma approch applied here assumes that the charged-particle energy produced in a neutron reaction will be deposited locally, i.e., within a negligible distance from the collision site or, more exactly, within one cell of the discrete-ordinates mesh.

The preliminary results for the total power deposited in the basic materials considered are given in Table III, normalized to the same volume of the SNQ facility building. One conclusion is that iron and concrete are able to absorb the largest amounts of the source energy. Water and graphite, however, are more sensitive to the maximum local density of the nuclear heating. The corresponding estimates of 400 kW of total power deposited in the shielding and a maximum power density of 1 W cm^{-3} were quoted in a previous report,[6] which also included

TABLE III

Total Energy Deposition in Kilowatts, by Neutrons and Gammas, in the SNQ Target Station Volume, Determined for Different Materials and Compared with the real Shielding Environment (beam energy, 1100 MeV; average beam current, 5 mA)

Contribution	Iron	Concrete	Earth	Graphite	Water	Real composition
Neutrons <20 MeV	11	76	27	38	143	21
Neutrons >20 MeV	133	116	54	63	46	117
Total gammas	150	70	29	27	17	106
Total	294	262	110	128	206	244
Maximum energy deposition (W-cm^{-3})	0.21	0.18	0.09	0.98	1.66	

TABLE IV

Total Neutron-Induced Radioactivity in the SNQ Target Station Volume, for Different Materials (Beam Energy, 1100 MeV; Average Beam Current, 5 mA)

Contribution	Induced radioactivity (kCi)		
	Air	Water	Graphite
Neutrons <20 MeV	5.30×10^{-3}	1.8	0
Neutrons >20 MeV	1.72×10^{-2}	14.2	26.0
Total	2.52×10^{-2}	16.0	26.0
Maximum local induced radioactivity ($kCi\text{-}cm^{-3}$)	2.10×10^{-5}	1.37×10^{-2}	2.18×10^{-2}

the high-energy proton contribution. Except in water, the high-energy neutron component exceeds the contributions from the low-energy neutrons and gammas. A similar comparison of the total and maximum radioactivity induced in the station volume is presented in Table IV. The light radioactive isotopes produced by spallation in air including ^{7}Be, ^{11}C, ^{13}N, ^{15}O, and ^{16}N are more important than the products of the low-energy neutron reactions. The radioactive products taken into account when considering air activation are listed in Table V, which also lists the maximum concentrations permitted by radiation protection regulations.[2] Although the radioactivity induced outside of the shielding seems not to be a serious problem, attention should be paid to the increase of this contamination caused by streaming effects through cracks or gaps in the bulk shielding and other leakage effects.

TABLE V

Maximum Induced Radioactivity in air, Inside and Outside the Station Beam Energy, 1100 MeV; Average Beam Current, 5 mA)

Isotope	Induced Radioactivity (mCi)		Permissible concentration
	Inside	Outside	
^{3}H	5.1×10^{6}	8.5×10^{-6}	2.0
^{7}Be	1.2×10^{5}	6.9×10^{-8}	6.0×10^{-3}
^{11}C	1.8×10^{6}	2.0×10^{-6}	8.0×10^{-3}
^{13}N	9.2×10^{6}	1.4×10^{-5}	5.0×10^{-3}
^{15}O	2.6×10^{6}	3.7×10^{-6}	3.0×10^{-4}
^{16}N	9.9×10^{5}	1.9×10^{-6}	5.0×10^{-4}

ACKNOWLEDGMENTS

One of the authors (JMZ) expresses his gratitude to the International Atomic Energy Agency for supporting his stay at the KFA Jülich and to the Director of the Institute of Reactor Development, Prof. R. Hecker, for supervising his training program. The authors are indebted to Mr. G. Sterzenbach for providing the HETC history tapes, to Dr. H. Schaal for making available other data and computer codes, and to Dr. K. Morstin for explaining some technical details concerning the DOT code operation.

REFERENCES

1. H. W. Patterson and R. H. Thomas, Eds., *Accelerator Health Physics* (Academic Press, New York, 1973), p. 437.
2. A. Rindi and R. H. Thomas, *Particle Accelerators* **7,** 23 (1975).
3. R. G. Alsmiller, Jr., *et al., Nucl. Instrum. Methods* **89,** 53 (1970).
4. R. G. Alsmiller, Jr., *et al., Particle Accelerators* **11,** 131 (1981).
5. K. Hayashi and T. Nakamura, *Nucl. Sci. Eng.* **87,** 123 (1984).
6. T. W. Armstrong, P. Cloth, D. Filges, and R. D. Neef, *Theoretical Target Physics Studies for the SNQ Spallation Neutron Source,* KFA report Jül–Spez–120 (1981).
7. T. W. Armstrong, P. Cloth, and D. Filges, "Computational Methods for High Energy Source Shielding," in *Proc. of the Sixth Meeting of the Intern. Collaboration on Advanced Neutron Sources,* Argonne National Laboratory report ANL–82–80 (1982).
8. P. Cloth, D. Filges, G. Sterzenbach, T. W. Armstrong, and B. L. Colborn, *The KFA Version of the High Energy Transport Code HETC and the Generalized Evaluation Code SIMPEL,* KFA Report Jül–Spez–196 (1983).
9. T. W. Armstrong, P. Cloth, D. Filges, and H. Schaal, "Calculational Methods and High Energy Cross Section for Spallation Source Shielding", in *Proc. of the Seventh Meeting of the Intern. Collaboration on Advanced Neutron Sources,* Chalk River Nuclear Laboratories report AECL–8488 (1983).
10. W. A. Rhoades, *et al., DOT. IV: Two-Dimensional Discrete Ordinates Radiation Transport Code System,* Oak Ridge National Laboratory report ORNL/TM–6529 (1978).
11. R. G. Alsmiller, Jr., F. R. Mynatt, J. Barish, and W. W. Engle, Jr., *Nucl. Sci. Eng.* **36,** 251 (1969).
12. J. M. Zazula, P. Cloth, D. Filges, and G. Sterzenbach, *Nucl. Instrum. Methods Phys. Res.* **B16,** 506 (1986).
13. R. G. Alsmiller, Jr., and J. Barish, *Neutron-Photon Multigroup Cross Sections for Neutron Energies* <400 *MeV,* Oak Ridge National Laboratory report ORNL/TM–7818 (1981).
14. W. B. Wilson, *Nuclear Data Development and Shield Design for Neutrons below* 60 *MeV,* Los Alamos National Laboratory report LA–7159–T (1978).
15. E. A. Belogorlov, V. T. Golowachik, V. N. Lebedev, and E. L. Potjamkin, *Nucl. Instrum. Methods* **199,** 563 (1982).
16. Radiation Shielding Information Center, *MACKLIB–IV*: 171 *Neutron,* 36 *Gamma-Ray Group Nuclear Response Function Library Calculated with MACK–IV from Cross-Section Data in ENDF/B–IV,* Argonne National Laboratory report ANL/FPP/TM–106 (1978).